This is a preprint, the final version is subject to change, of the American Mineralogist (MSA)
Cite as Authors (Year) Title. American Mineralogist, in press.
(DOI will not work until issue is live.) DOI: http://dx.doi.org/10.2138/am-2016-5769

Radionuclide Removal by Apatite

Revision 1: 6/15/2016

Mark J. Rigali, Patrick V. Brady and Robert C. Moore,

Sandia National Laboratories

Albuquerque, New Mexico 87185-0754

ABSTRACT

A growing body of research supports widespread future reliance on apatite for radioactive waste cleanup. Apatite is a multi-functional radionuclide sorbent that lowers dissolved radionuclide concentrations by surface sorption, ion exchange, surface precipitation, and by providing phosphate to precipitate low solubility radionuclide-containing minerals. Natural apatites are rich in trace elements, and apatite's stability in the geologic record suggest that radionuclides incorporated into apatite, whether in a permeable reactive barrier or a waste form, are likely to remain isolated from the biosphere for long periods of time. Here we outline the mineralogic and surface origins of apatite-radionuclide reactivity and show how apatites might be used to environmental advantage in the future.

Introduction

Calcium phosphate apatites, $Ca_{10}(PO_4)_6(F,OH,Cl)_2$, including fluorapatite, hydroxyapatite, and chlorapatite are collectively the tenth most abundant mineral on earth and its most abundant phosphate mineral (Hughes, 2015). While it is a common mineral, Hughes (2015) observes it is uncommonly versatile. It is the primary source of phosphate for fertilizer to feed human

populations and it makes up human bone and teeth. For these reasons alone it is one of the most important materials to mankind. Apatite is a key component in fluorescent lighting, a source material for phosphate detergents, a gechronometer, a gemstone and a laser material (Rakovan and Pasteris 2015). With a capacity to hold more than half of the long-lived elements of the periodic table in its structure (Hughes and Rakovan, 2015), and a structure that allows both cationic and anionic solid solutions and substitutions, apatite is also a versatile material for the field of environmental remediation (Rakovan and Pasteris, 2015).

Apatite can be used in permeable reactive barriers (PRBs) to isolate groundwater radionuclides, and as a waste form in planned nuclear waste repositories. Table 1 identifies the most common environmental radionuclides of concern and their sources. Phosphorous from dissolving apatite can remove a significant number of these radionuclides from solution by forming insoluble radionuclide-containing solids. Apatite surfaces sorb/exchange dissolved radionuclides, particularly cationic radionuclides including Sr, U, Pu, and Np, removing them from solution (Moore et al., 2002). In addition, U and Th are also known to be incorporated into apatites through a coupled substitution with SiO_4^{4-} and PO_4^{3-} (Terra and Audubert., 2006; Terra and Dacheux., 2006 and Terra et al., 2007). Apatite surfaces can also exchange anionic radionuclides for surface phosphate and/or hydroxyl groups to significantly lower dissolved levels of anionic radionuclides including $^{129}IO_3^-$ (Campayo et al., 2011; Coulon et al., 2014; and Laurencin et al., 2014) and $^{99}TcO_4^-$ (Moore et al., 2002 and Duncan et al., 2012)

Apatite PRBs are presently used to remove dissolved uranium and ^{90}Sr (see below). PRBs are a relatively simple, passive treatment technology for separating and immobilizing contaminants from groundwater. A reactive or sorptive media is placed perpendicular to the path of contaminated groundwater and down-gradient. Contaminants are removed upon contact with the

barrier. Conventional construction methods for permeable reactive barriers include trenching followed by backfilling with a reactive media, or high pressure injection of the media.

Because it can incorporate both anionic and cationic radionuclides, apatite has potential as a radioactive waste form (Boyer et al., 1997; Ewing 2001; Ewing and Wang, 2002; Guy et al., 2002; Dacheux et al., 2004; Duncan et al., 2012) or an engineered barrier in a nuclear waste repository (Krejzler, 2003 and Omel'yanenko, et al., 2007). Cationic radionuclides exchange for Ca^{2+} in apatite waste forms (e.g. Montel, 2011), in apatite formed *in situ* by phosphate amendments (Oelkers and Montel, 2008), and in phosphate-based cements (Leroux and Lacout, 2001). The fact that apatite has been stable for millions of years in numerous near surface environments (Gorman-Lewis et al. 2009) suggests that it can maintain radionuclide isolation from the environment for long periods of time (Horie et al, 2008). Furthermore, apatites demonstrate self-annealing and chemical durability to the damage resulting from α-decay events emitted from actinide radionuclides (Ochani et al., 1997; Ewing, 2001; Soulet et al., 2001; Chaumont et al., 2002; Livshits 2006; and Lu et al., 2013).

Our goals here are to: describe the solubility and sorptive behavior of apatite, identify the specific mechanisms of apatite uptake of individual radionuclides; and review the application of apatites for environmental radionuclide control.

Mineralogy and Solubility

Apatite is made up of a three dimensional network of PO_4 tetrahedra linked with a column of nine-fold coordinated Ca atoms (Ca1 site) (McConnell, 1938; Frank-Kamenetskaya, 2008). There are channels passing thru the phosphate network that have axes coinciding with six fold

screw axes and contain the triangles of seven fold coordinated Ca atoms (Ca2 site) and OH^-, F^-, or Cl^- ions (Frank-Kamenetskaya, 2008). Apatite forms hexagonal crystals and belongs to the *P63/M* space group.

The chemical composition, and solubility, of apatite varies; Cl^- and/or OH^- can substitute for F^-. Divalent cations such as Mg^{+2}, Sr^{+2}, and Ba^{+2} are able to substitute for Ca^{+2}. For example, strontiapatite, $Sr_{10}(PO_4)_6(OH)_2$, which is formed by the substitution of calcium by strontium is approximately 10^7 times less soluble than hydroxyapatite (Verbeeck et al., 1977). Strontium substitution in natural apatites is as high as 11% (Belousova et al. 2002) and can be as high as 13% and potentially higher in biologically precipitated apatite (Szecsody et al., 2009). In fact, biological precipitation is critical to the formation and performance of an in situ apatite barrier deployed on the Hanford reservation to prevent a Sr^{90} plume from reaching the Columbia River (discussed in detail below).

Paired substitutions allow incorporation of cationic rare earth elements (REE) into the apatite structure (Hughes and Rackovan, 2015). In other words, a trivalent REE cation must be paired with another substitution in order to maintain charge balance. This can occur in two ways: (1) $Na^+ + REE^{3+} \leftrightarrow 2Ca^{2+}$ and (2) $Si^{4+} + REE^{3+} \leftrightarrow P^{5+} + Ca^{2+}$. Such substitutions are common in natural apatites and significant because they can occur to the extent that apatite deposits (phosphates) approach ore grades for REEs. Further, natural REE-bearing mono-silicate-apatites (britholites) are stable for geologically significant periods of time (Carpena et al., 2001) and are also potential radioactive waste forms (Dacheux, et al., 2004).

Silicate, sulfate, carbonate, vanadate, arsenate, chromate, and several other oxyanions can substitute for PO_4^{-3} in apatite. (Pan and Fleet, 2002)$^{-}$. Carbonate can substitute for both phosphate and OH^-. Furthermore, carbonate substitutions into apatite structure can increase the reactivity of apatites (Frank-Kamenetskaya, 2008). Table 2 lists end-member metal phosphate solubilities.

Figure 1 shows pH-dependent hydroxyapatite solubility and aqueous phosphate speciation. Metal phosphate minerals in general have a minimum solubility at high pH where aqueous phosphate groups are highly anionic. The Y-coordinate of the solubility curve for the particular metal phosphate depends on the free energy of formation of the particular solid. The X-axis pH trend largely reflects aqueous speciation of the phosphate ion. Figure 2 shows the solubility of uranium (VI) phosphates, Na-Autunite ($Na_2(UO_2)_2(PO_4)_2$), Autunite ($Ca(UO_2)_2(PO_4)_2$), and $UO_2)_3(PO_4)_2{\cdot}4H_2O$, as a function of pH. It should be noted that Chernikovite $(H_3O)_2(UO_2)_2(PO_4)_2{\bullet}6(H_2O)$, a uranium phosphate phase that can form in the presence of calcium phosphate apatite PRBs is not represented in Figure 2 but is discussed below. The very low solubilities of many metal phosphates make phosphate and phosphate minerals good stabilizing agents for contaminant metals in soils (e.g. Zhang and Ryan, 1998, Manecki et al. 2000; Conca and Wright, 2006). The stability of the metal phosphate formed depends on the crystallinity and minor element chemistry of the metal phosphate solid formed and occasionally on the presence of a seed (Conca and Wright, 2006).

Surface Chemistry

The apatite surface is mostly made up of exposed Ca^{+2} and phosphate groups whose pH-dependent speciation parallels that of the respective aqueous species. Hydroxyapatite surfaces are anionic above pH ~ 8 and cationic below (e.g. Bengtsson, et al. 2008). A preliminary model of pH-dependent apatite surface speciation is shown in Figure 2. Figure 2 was constructed using the results of Bengtsson et al. (2008) using the surface complexation constants listed in Table 3. The model predicts that $>CaOH_2^+$, $>PO_3H^-$, and $>PO_3HCa^+$ are the dominant apatite surface species.

Cation and anion exchange reactions are obviously also important, e.g.

$$>CaOH_2^+ + Sr^{+2} \leftrightarrow >SrOH_2^+ + Ca^{+2} \qquad \text{[Cation Exchange]}$$

$$>PO_3H^- + CO_3^{-2} \leftrightarrow >CO_3H + PO_4^{-3} \qquad \text{[Anion Exchange]}$$

There appears to be a link between apatite surface charge and the extent of exchange. For example, Smiciklas et al. (1999) showed that Sr^{2+} exchange on hydroxyapatite is greater at high pH where the surface is negatively charged. Historically, apatite research has focused on establishing the chemistry of specific contaminants at the apatite surface for particular applications – PRBs, waste forms, and so on. The review below does likewise.

Apatite and Radionuclide Cations

Uptake of U and Sr by apatite has recieved the most attention; less so Np, Am, Pu, Co and other radionuclides. However, members of this latter group are also readily taken up by apatite as described below.

Uranium

Uranium concentrations in phosphate rock range from 3 to 400 mg/kg (e.g. Altschuler et al. 1958, Mortvedt, 1991). Additionally, uranium phosphates such as autunite are common in rocks and sediments as they are insoluble and stable under most environmental conditions (Gorman-Lewis et al. 2009). Although indirect, the examination of these analogs clearly suggest uranium apatites and uranium phosphates are stable for geologically significant periods of time and point to the long-term sequestration of uranium in these matrices. Direct experimental (Dacheux et al., 2004 and Terra, et al., 2006) and theoretical (Raicevic et al., 2006) studies demonstrate the stability of uraniferous apatites. In addition to the chemical stability of uraniferous apatites, their resistance to radiation damage as a result of the ability to self-heal also renders these apatites stable and able to hold uranium for long periods of time (Ouchani et al. 2007).

Uranyl ion, UO_2^{+2}, uranyl hydroxides, and uranyl carbonates are the primary forms of dissolved uranium in many soil solutions and waste environments. Apatite uptake of uranyl species apparently involves sorption, surface complexation (e.g. Bowie and Atkins, 1956), substitution into the apatite structure by ion exchange, and the formation of sparingly soluble uranium phosphates through various dissolution-precipitation mechanisms (Jeanjean et al. 1995). Dissolution-reprecipitation is the most important of these mechanisms and uptake depends upon pH, solution composition and the presence of other substitutions in the apatite (Smiciklas et al. 2008).

Chatelain et al. (2014) proposed a dissolution-reprecipitation mechanism in the formation of an amorphous uranium phosphate phase by the reaction of uranyl ions in the presence of biomimetic apatite. Krestou et al. (2004) observed dissolution-reprecipitation uptake of uranium by apatite dissolving to form $CaUO_2PO_4$ and/or $CaUO_2(CO_3)_2$, both of which are stable in acidic and neutral media. In addition, their kinetic experiments demonstrated rapid uptake of uranium by

apatite, occurring in minutes to hours. Arey et al. (1999) showed that addition of hydroxyapatite to uranium-contaminated sediment (1703 - 2100 mg/kg U) reduced dissolved uranium concentrations to below the drinking water standard (30 μg/L). Seaman et al. (2001) demonstrated similar hydroxyapatite immobilization of U in uranium-contaminated sediment. Raicevic et al. (2006) measured U uptake by soil amendments of hydroxyapatite, North Carolina Apatite, Lisina Apatite and Apatite II (a product made from fishbone) and showed that U immobilization depends on the chemical composition of the apatite. Simon et al. (2008) measured U uptake with long-term and radiotracer column experiments showed that uranium phosphate uptake altered the apatite structure but resulted in a stable solid phase. Wellman et al. (2008) showed that U was immobilized through surface complexation followed by formation of uranium phosphates.

Moore et al. (2002, 2004) grew apatite in soils using a calcium citrate and sodium phosphate solution to form finely distributed apatite. Citrate is a strong and stable chelator for calcium in the presence of phosphate and prevents the immediate formation of apatite from in calcium citrate and sodium phosphate solutions. Once the solution is placed in sediment, the indigenous soil microogranisms degrade the citrate and then the calcium reacts with the phosphate to precipitate apatite in the sediment. Phosphate serves two roles; it buffers solution pH to ~7.2 which favors formation of apatite over other calcium phosphates that sorb less. Figure 4 shows the formation of apatite in a solution inoculated with soil bacteria. Moore (2002, 2004) showed that soils containing in situ precipitated apatite decreased dissolved U by 89 to 99% whereas dissolved uranium concentrations decreased by 62 to 91% in apatite-free soils. However apatite-containing soil desorbed 1% or less of the sorbed uranium while apatite-free soil released 31 to 35% of the sorbed uranium.

Strontium

Dissolved Sr exists as Sr^{+2} below pH ~ 9 in soil solutions and waste environments. Under alkaline conditions $SrCO_3^{aq}$ is more abundant. Lazic and Vukovic (1991) showed Sr adsorption onto synthetic hydroxyapatite occurs by ion exchange between Sr^{+2} and Ca^{+2}. Ravicevic et al. (1996) determined a maximum sorption capacity of $3.8 \pm 0.3 \times 10^{-2}$ mol Sr/mol P for a poorly crystalline hydroxyapatite. Moore et al. (2002) measured ^{90}Sr sorption by hydroxyapatite formed in sediment using the apatite-forming solution described above and demonstrated that average Sr uptake ranged from 19.5 to 94.7% for a treated soil and 34.2 - 4.8% for an untreated soil. Smiciklas et al. (2005) measured Pb, Cd, Sr, and Zn uptake capacities to be Pb > Cd > Zn > Sr independent of apatite composition, crystallinity, specific surface area, points of zero surface charge and sorption capacities. The same order was obtained for both single metal solutions and their mixture. A linear relationship between the amount of metals sorbed and Ca^{2+} released from HAP was observed for all the metal ions. The work of Smiciklas et al. (2005) also suggests that apatite could also be effective at remediating heavy metal soil and sediment contamination in addition to radionuclides.

Kurgan et al. (2005) used electron microscopy, x-ray analysis, IR-spectroscopy, proton nuclear magnetic resonance and radiometry, to demonstrate that nanosize and poorly crystalline hydroxyapatite crystals have a high sorption capacity for H_2O and ^{90}Sr. The distribution coefficient (K_d), defined as the amount of ^{90}Sr distribution between the apatite and the solution, does not depend on the radionuclide concentration within the range of 4.2-61 Bq/ml. However, ^{90}Sr desorption was directly proportional to the radionuclide concentration in solution. It was demonstrated that desorption of ^{90}Sr could be reduced by a factor of 30 with a negligible reduction

of K_d. simply by annealing the poorly crystalline hydroxyapatite at 650° C to transform it to a highly crystalline state.

Sasaki et al. (2012) measured ^{90}Sr sorption by calcined catfish bones treated at 400 - 1100°C to remove organic matter (87.1 mg/g). Bone treated at higher temperatures exhibited an increase in crystallinity as indicated by a decrease in lattice strain, 0.0098 to 0.00135, together with an increase in crystallite sizes, 5.0 x 10^{-8} to 7.7 x 10^{-8} m. A decrease in the specific surface area from 98.9 to 0.99 m^2/g and an increase in the particle size, 50 to 1000 nm were also observed. The sorption densities of Sr^{2+} decreased with increasing calcination temperatures, from 0.34 to 0.05 mmol/g. Lower calcination temperatures produced amorphous hydroxyapatite, which released more aqueous phosphate, resulting in the precipitation of strontium phosphates.

Park et al. (2002) measured apatite formation of by precipitation in the presence of dissolved Sr and Cs. Sr and Cs are both taken into the apatite structure. Even while Sr was removed from solution more effectively than Cs, this has important implications for treating Cs and Sr-bearing waste streams and contaminated soils.

Other Cationic Radionuclides

Thomson et al. (2003) measured sorbent removal of low levels of actinides, particularly Pu, U, and Am, and hazardous metals. Nine sorbents were tested including natural and synthetic apatites, tri-calcium phosphate, and bone char. Moderate sorption of As, Se, Sr, Cs, and Tc and very good removal of U and Pu by the phosphate adsorbents were observed. The Am results were inconclusive. The authors also established that synthetic apatites had higher capacities for the radionuclides studied than natural apatites (phosphate rock and fish bones).

Moore et al. (2005) measured sorption of Pu(VI) by synthetic hydroxyapatite in $NaClO_4$ media to be rapid with equilibrium attained in 2 hours. Sorption was pH dependent with distribution constants, log K_d values (in ml/g), ranging from 4.11 at pH 6 to 5.92 at pH 8.5. Data collected at pH 8.0 with varying total Pu(VI) were fit well with a Langmuir isotherm and yielded Langmuir constants of C_a = 0.0147 mole/mole and $K = 1.71 \cdot 10^8$ l/mole. Although varying ionic strength did not have an effect on Pu(VI) sorption, a decrease in sorption was evident at high calcium and phosphate concentrations.

NpO_2^+ to synthetic hydroxyapatite is also fast with sorption of initial concentrations of Np(V) concentration of 1 x 10^{-7} to 1 x 10^{-6} M reaching equilibrium in ~ 3 hours (Moore et al. 2003). Sorption is strongly pH dependent with distribution coefficients increasing from 123 L/mole at pH 6 to 69,200 L/mole at pH 8.5. Data collected at pH 8.0 over a range of Np(V) concentrations were well fit with a Langmuir isotherm model for simple adsorption. Langmuir parameters were determined to be C_a = 0.032 mole/mole and K = 1.22 x 10^6 L/mole, indicating the high affinity of hydroxyapatite for Np(V) adsorption.

Thakur et al. (2006) measured NpO_2^+ sorption on hydroxyapatite as a function of the amount of sorbent, initial NpO_2^+ concentration, ionic strength and pcH. At ionic strengths of 0.10 to 5.00M $NaClO_4$, sorption increased with increased pcH to a maximum between pcH 8-8.5, then decreased as the pcH increased. The kinetics of NpO_2^+ sorption on hydroxyapatite followed Lagergren first order kinetics. The temperature dependence of sorption was small in the range of 273-283 K, but increased more sharply at higher temperatures of 298-333 K. The heat of sorption of NpO_2^+ was endothermic and the free energy values were exothermic indicating large, positive entropy. The activation energy for the sorption process was calculated to be 29.5 ± 1.2 kJ/mole.

Smiciklas et al. (2006) measured the sorption of Co^{2+} by synthetic hydroxyapatite in batch experiments as a function of initial metal concentration, equilibration time, solution pH and presence of EDTA. The sorption process followed pseudo second-order kinetics with 24 hours required to reach equilibrium. Co^{2+} uptake was quantitatively evaluated using the Langmuir and Dubinin–Kaganer–Radushkevich (DKR) model. The Langmuir adsorption isotherm constant corresponding to adsorption capacity was found to be 20.92 mg/g. Sorption of Co^{2+} was constant in the initial pH range 4–8. However, in the presence of EDTA, sorption of Co^{2+} decreased due to the formation of Co-EDTA complexes with lower sorption affinities for hydroxyapatite.

Th is a common substituent in natural apatites and is stable in its structure. Th can be retained within apatites for geologically significant periods of time. For example, it is present in the hydrothermal apatites associated with the 2Ga old Oklo natural reactors. (Bros et al., 1996). It has been established that it incorporates into synthetic apatites, in particular the silicate-bearing apatite known as britholite (Terra, et al., 2006). In this study dry phase incorporation of Th was achieved into the britholoite structure. This was achieved through a process of mechanical grinding of a thorium oxide- or thorium phosphate-britholite mixture followed by a heat treatment at 1400 C for 6 hours.

A study by Bostick (2003) demonstrated that apatite has a strong ability to remove soluble thorium, in part by the formation of a thorium phosphate particulate phase. Thorium, as hydrous thorium nitrate, $Th(NO_3)_4 \cdot nH2O$, was added to synthetic groundwater in the presence of bone apatite. The resulting solution had a pH of 3.3 and a fine silt-like precipitate formed on the surface of the apatite. X-ray Spectroscopy (SEM-EDS) established that this precipitate was an unidentified Th-rich calcium phosphate solid phase.

With respect to Ra^{2+}, it is present in apatite in secular equilibrium with uranium (Menzel, 1968). While there are few studies of Ra uptake by apatite in the literature, a study by Neuman et al, 1955 demonstrated that Ra^{2+} will readily substitute for Ca^{2+} in hydroxyapatite. It has also been shown to remediate Ra. When typical waste effluents from a uranium mine are treated with apatite, radium-leach values are reduced to levels below 0.1 pCi/L (Murray et al., 1983). In light of the recent concerns associated with significant quantities radium in produced and fracking waters, (Benevides et al., 2015), apatite sorbents and PRBs should be investigated for their potential to remediate this radionuclide.

Apatite and Radionuclide Anions

Pertechnetate, TcO_4^-, and iodide, I^-, are problematic radionuclide anions in soil fluids and waste environments because they are less likely to sorb to anionic mineral surfaces. Tc exists as TcO_4^- under oxidizing conditions while under reducing conditions Tc forms insoluble solids. Under highly oxidizing conditions I forms iodate, IO_3^-. Other radioactive anionic species such as those of Se include selenate, SeO_4^{2-}, and selenite, SeO_3^{2-}, and are of lesser radiochemical concern. The apatite mineral group is one of the rarer examples of a mineral group that allows for anion solid solutions and substitutions (Hughes and Rakovan, 2015), and there is considerable evidence that both anions and oxyanions sorb to apatite surfaces. Oxyanions including CO_3^{2-}, SO_4^{2-}, VO_4^{3-}, AsO_4^{3-}, SeO_3^{2-}, SeO_4^{2-}, IO_3^-, and TcO_4^- can sorb and potentially even replace PO_4^{3-} in the apatite structure (Narasaraju and Phebe 1996; Moore et al. 2002; Duc et al. 2003; Bostick, 2003; Lee et al. 2009; Lee, 2010; Campayo et al. 2011; Duncan et al., 2012).

Pertechnetate

Because it is an abundant fissiogenic isotope and it has a long half-life (2.1 x 10^5years) ^{99}Tc is the major driver for the long term dose risk at both the DOE Hanford and Savannah River

nuclear reservations. A chemically modified hydroxyapatite known as stannous hydroxyapatite has proven to be extremely effective at reducing, capturing and sequestering pertechnetate (TcO_4^-) (Moore et al. 2002). Combined reduction and incorporation causes permanent sequestration of Tc into the apatite lattice (Duncan et al. 2012, Cooke et al. 2008). Furthermore, the reoxidation of the Tc appears to be inhibited by the presence of tin in the apatite structure (Duncan et al. 2012). The authors also report that phosphate is released into solution during the process of Tc incorporation suggesting TcO_4^- can sorb and potentially replace PO_4^{3-} in the apatite structure. Although the mechanism is uncertain, it is presumed that an exchange reaction takes place and the captured technetium is sequestered within the stannous hydroxyapatite and is therefore very resistant to re-oxidation.

Iodide/Iodate

Phebe and Narasaraju (1995) demonstrated that a solid solution exists between hydroxyapatite $Ca_{l0}(PO_4)_6(OH)_2$ and iodoapatite $Ca_{l0}(PO_4)_6(I)_2$ establishing that iodide will readily substitute for hydroxide in the hydroxyapatite structure. Other related apatite compositions such as the lead vanadophosphate iodine apatite, $Pb_{10}(VO_4)_{4.8}(PO_4)_{1.}2(I)_2$, synthesized by Campayo et al. (2015) are known to exhibit high chemical durability making them attractive as a waste form for the immobilization of radioactive iodine.

Laurencin et al. (2014) measured incorporation of iodate in Ca-hydroxyapatite and Sr-hydroxyapatite lattices. On one hand, I K and L-3-edge X-ray Absorption Near Edge Structure spectra are indicate that while the local structure around the iodate is similar in the two substituted hydroxyapatite lattices, it differs significantly from the one observed in a series of model compounds including $NaIO_3$, KIO_3, and $Ca(IO_3)_2{\cdot}H_20$. I K-edge Extended X-ray Absorption Fine Structure spectra were analyzed and revealed a lack of order around the

iodate, and also the absence of local clustering of the iodates along the hydroxyl columns of the apatite.

Coulon et al. (2014) describes a cementation synthesis process for iodate-substituted hydroxyapatite. The material is obtained from a mixture of tetracalcium phosphate (TTCP), tricalcium phosphate (aTCP) and sodium iodate ($NaIO_3$), taken in a molar ratio of 1/2/0.5. Sodium iodate acts as a set retarder, by leading to the precipitation of non-cohesive transient phases, which are then destabilized when the massive precipitation of hydroxyapatite occurs. The setting time of the waste form was controlled by adding hydroxyapatite seeds to the cement paste. This cementitious system leads to a porous material composed of iodine-substituted hydroxyapatite needles covering residual TTCP and aTCP particles. Iodine is present in the hydroxyapatite structure as iodate anions only and the authors conclude that it substitutes primarily for hydroxyl groups as opposed to phosphate groups. An iodine incorporation rate of 6.5 wt% was obtained using the authors system.

Selenate/Selenite

Besides its presence in natural systems, selenium is also present in small quantities in high level waste as the long-lived radionuclide ^{79}Se with a half-life of 6.5 x 10^4 years. Sorption and incorporation behavior of selenite species on hydroxyapatite has been repeatedly observed (Montiel-Rivera et al. 2000; Duc et al. 2003; Lee, 2010; Ma et al. 2013; Kolmas et al. 2014; Kolmas et al. 2015; Moore et al. in review). Monteil-Rivera et al. (2000) showed that selenite substitutes into the apatite structure for phosphate and that substituted selenium is located at the surface as well as diffused into the structure of the hydroxyapatite. Duc et al. (2003) measured sorption of selenium by hydroxyapatite, fluorapatite and iron oxides and found sorption of selenite by hydroxyapatite to be pH-dependent with the highest uptake occurring at a pH of

approximately 8. Sorption by fluorapatite was not significantly affected by pH but the total uptake of selenium was 2 to 3 orders of magnitude less than that measured for hydroxyapatite. The mechanism for selenium uptake is adsorption of selenite followed by substitution for phosphate in the hydroxyapatite. However, the kinetics of selenite uptake by hydroxyapatite are very slow requiring more than 100 hours to reach equilibrium suggesting that for systems with rapid groundwater flow, a permeable reactive barrier would not be practical as a remediation option. More recently, Moore et al. (in review) have demonstrated that carbonated hydroxyapatite can accelerate the rate of sorption of selenite and its substitution into the apatite structure. They demonstrated selenite uptake can reach equilibrium in as little as 5 hours. Together these studies suggest that the rate, amount and perhaps even the mechanism of selenite uptake by hydroxyapatite can be significantly affected by changing or 'tuning' the composition and structure of the hydroxyapatite sorbent.

Fewer studies have examined sorption and incorporation of selenate on hydroxyapatite (Montiel et al. 2000; Duc et al. 2003; Lee 2010; Kolmas et al. 2014; Kolmas et al. 2015). When compared to selenite, selenate uptake appears to be much less significant and some cases negligible (Duc et al. 2003). While hydroxyapatite shows little affinity for selenate it may be possible to dope hydroxyapatites with a redox sensitive cation such as Sn (II) for calcium to increase uptake. The stannous hydroxyapatite could potentially take up selenate by (1) reduction to selenite by the incorporated Sn (II) followed by (2) uptake of the arsenate as arsenite. Such a mechanism has been proposed for pertechnatate uptake by stannous apatite as described above.

Apatite-Radionuclide Field Applications

Apatite has been incorporated into several permeable reactive barriers, most notably ones at: Fry Canyon, UT, for U; at the Hanford 100-N area for ^{90}Sr; and at Fukushima in Japan for ^{90}Sr, each using a different form of apatite.

Fry Canyon

Fry Canyon is located in southeastern Utah and is a former site where uranium and copper ores were processed. A plume of contaminated groundwater lies beneath the Fry Canton site containing concentrations of dissolved uranium of 1,000 to 20,000 micrograms/L (Otton et al, 2010). Six permeable reactive barriers were installed at Fry Canyon and operated from September 1997 through December 1999. Two methods for deployment of the barriers and three reactive media, including bone char phosphate, were investigated for their ability to sequester uranium in the groundwater. The main constituent of the bone char was apatite. The bone char was effective at removing 88.1% of the uranium passing through the barrier (Naftz et al. 2000).

Fuller et al. (2003) examined bone char samples retrieved from the permeable reactive barrier by EXAFS. The analysis indicated U(VI) uptake by the bone char phosphate was through surface complexation for sorbed concentrations of $\leq$ 5500 μg U/g apatite. At sorbed uranium concentrations of $\geq$ 5500 μg U/g apatite, the uranyl phosphate chernikovite ($(H_3O)_2(UO_2)_2(PO_4)_2 \cdot 6(H_2O)$) with a solubility constant of 1.8 x 10^{-23} (Haverbeke et al. 1996). was formed. However, the presence of carbonate at a concentration of 4.8 mM in the groundwater suppressed the formation of chernikovite and at sorbed uranium concentrations of up to 12,300 μg U/g apatite and reduced the effectiveness of U uptake.

Hanford 100-N Site

The Hanford 100-N site is adjacent to the Columbia River in Western Washington on the Department of Energy Hanford Reservation where plutonium for nuclear weapons was produced in large quantities. The primary source of ^{90}Sr contamination is from liquid waste disposal in a trench near the Columbia River. The 100-N site is located on a plateau slightly above and adjacent to the river and is contaminated with ^{90}Sr. The Vadose zone at the 100-N site is 0 to 23 m thick and is composed of gravels and sands of the Hanford and Ringold Formation. The unconfined aquifier is approximately 6.5 to 14 m thick. When the Columbia River stage is high the water table can rise into the Hanford formation. A 90 meter permeable reactive barrier was placed in sediment adjacent to the Columbia River. The barrier was constructed over a two year timeframe from 2006 to 2008 using the previously described apatite-forming solution (Moore et al. 2003). Sixteen wells were used to inject the solution into the sediment creating an overlapping, continuous permeable reactive barrier. As of 2014, the barrier is meeting or exceeding the treatment objective of a reduction in Sr^{90} concentrations of 90% as measured down gradient of the barrier (Vermuel et al., 2014). As of 2016 the DOE has plans to expand the barrier to protect a 300 m stretch of the Columbia River.

Fukushima

The Fukushima site is located on the east coast of Honshu Island in northeastern Japan on Cenozoic sedimentary rock. It is separated from the adjacent Abukuma granite plateau by the Futuba fault. The plant sits on “mudrock” type sedimentary rock which is muddy rock composed of clay and silt. (Fetet, 2011). Groundwater contaminated with ^{90}Sr and ^{137}Cs has been continuously removed from the site, the ^{137}Cs is being removed by ion exchange while the ^{90}Sr contaminated water is being stored until the ^{90}Sr can be removed. The contaminated water is currently being held in large above ground tanks. There have been several leaks from the

tanks resulting in the release of ^{90}Sr-contaminated water. In response to the spills, a permeable reactive barrier was placed in the path of the contamination. The barrier was constructed using a mixture of zeolite and processed pig bones (composed primarily of apatite). However, because the soil at Fukushima highly retards migration of Sr, it will be years before the Sr reaches the barrier and its performance can be evaluated (Ijiri 2014).

Research is ongoing for the construction of a second permeable reactive barrier at Fukushima. The proposed barrier will be constructed as a biogenic in situ apatite barrier through injection of a glycerol phosphate into the subsurface in the path of contaminated groundwater. Similar to the in situ barrier technology developed by Moore (described above) the indigenous soil microorganisms will be relied upon to degrade the glycerol phosphate allowing the phosphate to react with calcium in the sediment to produce apatite (Japan Association of Mineralogical Sciences, 2015)

Discussion

Apatite is capable of isolating a number of radionuclides that are of environmental concern, and has the potential application as a PRB and a waste form. Apatite PRBs have been successfully demonstrated in the field and they have several advantages over most other groundwater remediation approaches. Once a groundwater plume has been remediated by passing completely through a PRB, the PRB and contaminant can be removed and disposed of elsewhere. Alternatively, a PRB that has remediated a radionuclide plume can be left in place until the radionuclide has decayed.

Furthermore, construction of an apatite PRB using the apatite-forming solution developed by Moore et al., 2002 has many advantages over other conventional construction including:

- The barrier is simple and inexpensive compared to trenching and uses nonhazardous chemicals
- With the exception of monitoring, there are no operational expenses for the barrier once in place
- Worker exposure to contaminants is minimal as compared to above-ground ex situ treatment technologies, and
- Disposal costs for contaminated soil generated by removal are eliminated and no waste streams are generated.

Physical and chemical conditions advantageous for use of the apatite-forming solution to create a permeable reactive barrier include:

- Sufficiently high soil permeability to permit the apatite-forming solution to spread out both horizontally and vertically
- A pH between 6.9 and 9.0
- A relatively slow groundwater flowrate to allow apatite formation before the apatite forming solution can be washed out of the injection site. The specific flow rate will depend on the particular site since many site-specific factors affect apatite formation including groundwater temperature, microorganism activity, and groundwater composition.
- An active microbial population for degradation of the citrate.

Implications

Apatite PRBs are poised to play an ever larger role in radionuclide removal from the environment. In particular, an apatite PRB might be used as part of the multi-barrier concept that most nuclear waste repositories use. Not only does apatite sorb/sequester long-lived radionuclides, it is also redox insensitive, and its presence does not notably alter the bulk geochemistry of the repository environment.

Apatite has a special advantage over "advanced waste forms" assembled of exotic materials and methods. The persistence of apatite in the geologic record allows its effectiveness as a waste form to be qualitatively predicted. Conversely, advanced waste forms for which there is no long term "track record" cannot be relied on heavily for long-term radionuclide isolation. That being said, greater confidence in apatite performance requires answering the following questions through more extensive research.

How do multiple radionuclides interact at the apatite surface? Most experiments have focused on single radionuclides because they were often designed to test a PRB sorbing a single radionuclide. Apatite in a repository backfill will "see" many radionuclides simultaneously, along with the dissolved species in the ambient groundwater. Developing an experimental and theoretical understanding of how multiple species interact at the apatite surface is needed. This effort will also help sort out the relative contributions of surface complexation and exchange.

What are the chemical controls over apatite dissolution-reprecipitation? Dissolution-reprecipitation particularly in surface layers is a strong control over apatite uptake of U. It has been established that autinite ($CaUO_2)_2$ $(PO_4)_2$) (Ohnuki et al., 2004) and chernikovite ($(H_3O)_2(UO_2)_2(PO_4)_2 \bullet 6(H_2O)$) (Fuller et al., 2003) can form on the surface of apatite most likely

through dissolution-reprecipitation mechanisms. The precise reaction pathway (e.g. sorption, incorporation or co-precipitation) is determined by numerous factors associated with groundwater chemistry (Mehta et al., 2016). Dissolution-reprecipitation probably plays an important role in other contaminant-apatite interactions well (e.g. Th as discussed above). Working out how the bulk apatite surface, and the species adsorbed/exchanged onto it, responds to groundwater chemistry is the key.

How does apatite react over the medium term? Lab experiments with apatite say something about 1 year chemical processes; natural apatites give information about > 1 million year processes. PRBs and nuclear waste backfills perform over time spans in between a year and a million years. Long-term tests, or short-term tests accelerated by temperature, are needed to give greater confidence in apatite performance over the medium term.

Acknowledgements

Sandia National Laboratories is a multi-program laboratory managed and operated by Sandia Corporation, a wholly owned subsidiary of Lockheed Martin Corporation, for the U.S. Department of Energy's National Nuclear Security Administration under contract DE-AC04-94AL85000. This work is supported by DOE Office of Nuclear Energy, Office of Used Nuclear Fuel Disposition and DOE Office of Legacy Management.

References

Altschuler, Z.S., Clarke, R.S., and Young, E.J. (1958) Geochemistry of uranium in apatite and phosphorite. Geological Survey Professional paper 314-D.

Arey, J., Seaman, J.C., and F.P. Bertsch, F.P. (1999) Immobilization of uranium in contaminated sediments by hydroxyapatite addition. Environmental Science and Technology, 33, 337-342.

Belousova, E.A., Griffin, W. L., O'Reilly, S. Y., and Fisher, N. I. (2002) Apatite as an indicator mineral for mineral exploration: Trace-element compositions and their relationship to host rock type. Journal of Geochemical Exploration, 76, 45-69.

Benavides P.T., Gebreslassis, B.H. and Diwekar, U.M. (2015) Optimal design of adsorbants for NORM removal from produced water in natural gas fracking: CAMD for adsorption of radium and barium. Chemical Engineering Science, 137, 977-985.

Bengtsson, A., Shchukarev, A., Persson, P, and Sjöberg, S. (2008). A solubility and surface complexation study of a non-stoichiometric hydroxyapatite. Geochemica et Cosmochimica Acta, 73, 257-267

Bostick, W.D. (2003) Use of apatite for chemical stabilization of subsurface contaminants. Final Report under contract DE-AC26-01NT41306. US Dept. of Energy, National Energy Technology Laboratory.

Boyer, L., Carpena, J., and Lacout, J.L. (1997) Synthesis of phosphate-silicate apatites at atmospheric pressure. Solid State Ionics, 95, 121-129.

Bowie, S.H.U and Atkins, D. (1956) An unusually radioactive fossil fish from Thrso, Scotland Nature, 177, 487-488.

Brady, P.V., Pohl, P.I., and Hewson, J.C. (2014) A coordination chemistry model of algal autoflocculation. Algal Research 5, 226-230.

Bros, R. Carpena, J. Sere, V., and Beltritti, A. (1996) Occurrence of Pu and fissiogenic REE in hydrothermal apatites from the fossil nuclear reactor 16 at Oklo (Gabon). Radiochimica Acta, 74, 277-282.

Campayo, L., A. Grandjean, A. Coulon, R. Delorme, D. Vantelon, and Laurencin, D. (2011) Incorporation of iodates into hydroxyapatites a new approach for the confinement of radioactive iodine, Journal of Materials Chemistry, 21, 17609-17611.

Campayo, L, Le Gallet, S. Perret, D., Courtois , E., Cau Dit Coumes, C., Grin, Yu., and Bernard, F. (2015), Relevance of the choice of spark plasma sintering parameters in obtaining a suitable microstructure for iodine-bearing apatite designed for the conditioning of I-129, Journal of Nuclear Materials, 457, 63-71.

Carpena, J., Boyer, L., Fialin, M., Kienast, J.R., and Lacout, J.L. (2001) Ca^{2+}, PO_4^{3-} = Ln^{3+}, SiO_4^{4-}coupled substitution in the apatite structure stability of the mono-silicated fluor-apatite. Earth and Planetary Science. Letters, 333, 373-379.

Chaumont, J., Soulet, S. Krupa, J.C., and Carpena, J. (2002) Competition between disorder creation and annealing in fluorapatite nuclear waste forms. Journal of Nuclear Materials 301, 122-128

J. Cooke G.A., Duncan, J.H., and Lockrem, L.L. (2008) Assessment of technetium leachability in Cement Stabilized Basin 43 groundwater brine. RPP-RPT-39195, Rev. 0, CH2M Hill Hanford Group, Inc., Richland, Washington.

Conca, J.L. and Wright, J. (2006) An Apatite II permeable reactive barrier to remediate groundwater containing Zn, Pb and Cd, Applied Geochemistry, 21,1288-1300.

Coulon, A., Laurencin, D., Grandjean, A., Coumes, C.C.D., Rossognol, S., and Campayo, L. (2014) Immobilization of iodine into a hydroxyapatite structure prepared by cementation. Journal of Materials Chemistry A 7(48). 20923-20932.

Dacheux, N., Clavier, N., Robisson A-C., Terra, O., Audubert, F., Latigue, J-E., and Guy, C. (2004) Immobilisation of actinides in phosphate matrices. Comptes Rendus Chimie 7, 1141-1152.

Duc, M., Lefevre, G., Fedoroff, M., Jeanjean, J., Rouchaud, J.C., Montiel-Rivera, F., Dumonceau, J., and Milonjic, S. (2003) Sorption of selenium anionic species on apatites and iron oxides from aqueous solutions. Journal of Environmental Radioactivity, 70, 61-72.

Duncan, J.A., Hagerty, K., Moore, W.P., Rhodes, R.N., Johnson, J.M., Moore, R.C. (2012). LAB-RPT-12-00001, Laboratory Report on the reduction and stabilization (immobilization) of pertechnetate to technetium dioxide using tin(II) apatite, Rev. 0, Washington River Protection Solutions, LLC, Richland, Washington.

Duncan, J.A., Cooke, G.A., and Lockrem, L.L. (2009) Assessment of technetium leachability in Cement-Stabilized Basin 43 groundwater brine 20RPP-RPT-39195, Rev. 1, Washington River Protection Solutions, LLC, Richland, Washington.

Ewing R.C. (2001) The design and evaluation of nuclear waste forms: clues from mineralogy. Canadian Mineralogist, 39, 697-715.

Ewing R.C. and Wang, Z., (2002) Phosphates as nuclear waste forms in M.J. Kohn, J. Rakovan and J.M. Hughes eds., Phosphates: Geochemical, Geobiological and Materials Importance, 48,

pp. 673-699. Reviews in Mineralogy and Geochemistry, Mineralogical Society of America, Chantilly, Virginia.

Fetet, P. (2011) The Geology of Fukushima. Posted in Le blog de Fukushima. November 12, 2011.

Frank-Kamenetskaya, O.V. (2008) Minerals as Advanced Materials I pp 241-252, Structure, chemistry and synthesis of carbonate apatites — The Main Components of Dental and Bone Tissues. Springer Berlin Heidelberg.

Fuller, C.C., Bargar, J.R. and Davis, J.A. (2003) Molecular-scale characterization of uranium sorption by bone apatite materials for a permeable reactive barrier. Environmental Science and Technology 37, 4642-4649.

Gorman-Lewis, D., Shvareva, T., Kubatko, K., Burns, P., Wellman, D., McNamara, B., Szymanowski, J., Navrotsky, A., and Fein, J. B. (2009) Thermodynamic properties of autunite, and uranyl orthophosphate from solubility and calorimetric measurements. Environmental Science and Technology 43, 7416-7422.

Guy, C., Audubert, F., Lartigue, J-E., Latrille, C., Advocat, T., Fillet, C. (2002) New conditionings for separated long-lived radionuclides. Comptes Rendus Physique, 827-837.

Horie, K., Hidaka, H., and Gauthier-Lafaye, F. (2008) Elemental distribution in apatite, titanate and zircon during hydrothermal alteration: durability of immobilization mineral phases for actinides. Physics and Chemistry of the Earth, 33, 962-968.

Hughes, J.M. (2015) The many facets of apatite. American Mineralogist, 100, p. 1033-1039.

Hughes, J.M. and Rakovan, J.F. (2015) Structurally robust, chemically diverse apatite and apatite supergroup minerals. Elements, 11, 165-170.

Ijiri, Y, General Manager, Nuclear Facilities Division, Taisei Corporation, Japan (personal communication, 2014).

Japan Association of Mineralogical Sciences (2015) Eliminating radionuclides in seawater at Fukushima Daiichi Nuclear Power Plant – The use of Halophilic Microorganisms. http://jams.la.coocan.jp

Jeanjean, J., Rouchaud, J.C., and Tran, L. (1995) Sorption of uranium and other heavy metals on hydroxyapatite. Journal of Radioanalytical and Nuclear Chemistry – Letters, 201, 529-539.

Kolmas, J. Oledzka, E., Sobczak, M. and Nalecz-Jawecki, G. (2014) Nanocrystalline hydroxyapatite doped with selenium oxyanions: a new material for biomedical applications. Materials Science and Engineering C, 39, 134-142

Kolmas, J., Kuras, M., Oledzka, E. and Sobczak, M. (2015) A solid-state NMR study of selenium substitution into nanocrystalline hydroxyapatite. International Journal of Molecular Science, 16, 11452-11464.

Krestau, A. and Panias, X. (2004) Mechanism of aqueous Uranium(VI) uptake by hydroxyapatite. Minerals Engineering, 17, 373-381.

Kurgan, N.A., Rozko, A.N., Kalinichenko, E.A., and Kalinichenko A.M. (2005) Adsorption of Sr-90 on nanoscale particles of hydroxylapatite. Metallofizikai Nobeishie Tekhnologi, 27, 1539-1549.

Laurencin, D., Vantelon, V. Briois, C. Gervais, C., Coulon, A. Grandjean, L. and Campayo, L. (2014) Investigation of the local environment of iodate in hydroxyapatite by combination of X-ray absorption spectroscopy and DFT modeling. Royal Society of Chemistry Advances, 4(28), 14700-14707.

Lazic, S. and Vukovic, Z. (1991) Ion exchange of strontium on synthetic hydroxyapatite. Journal of Radioanalytical and Nuclear Chemistry, 149, 161-168.

Lee, Y.J., Stephens, P.W., Tang, Y., Li, W., Phillips, B.L, Parise, J.B., and Reeder, R.J. (2009) Arsenate substitution in hydroxylapatite: structural characterization of the Ca5(PxAs1-xO4)3OH solid solution. American Mineralogist, 94, 666-675.

Lee, Y.J. (2010) Spectroscopic investigation of arsenate and selenate incorporation into hydroxylapatite. Current Applied Physics, 10, 158-163.

Leroux, L. and Lacout, J.L. (2001) Preparation of calcium strontium hydroxyapatite by a new route involving calcium phosphate cement. Journal of Materials Research 16, 171-178

Livshits, T.V. (2006) Britholites as natural analogues of actinide matrices: resistance to radiation damage. Geology of Ore Deposits, 48, 410-422.

Lu, F., Dong, Z., Zhang, J., White, T. Ewing R.C., and Lian, J. Tailoring the radiation tolerance of vanadate-phosphate fluorapatites by chemical composition control. RSC Advances, 3, 15178-15184.

Ma, J., Wang, Y., Zhou, L., and Zhang, S. (2013) Preparation and characterization of selenite substituted hydroxyapatite. Materials Science and Engineering C, 33, 440-445.

Manecki, M., Maurice, P.A., and Traina, S.J. (2000) Kinetics of aqueous Pb reaction with apatites. Soil Science, 165, 920-933.

McConnell, D.A. (1938) Structure investigation of isomorphism of the apatite group. American Mineralogist 23, 1-19.

Mehta, V.S., Maillot F., Wang Z., Catalano J.G., and Giammar, D.E. (2016) Effect of reaction pathway on the extent and mechanism of uranium (VI) immobilization with calcium and phosphate. Environmental Science and Technology, 50, 3128-3136.

Menzel, R.G. (1968) Uranium, Radium, and Thorium Content in Phosphate Rocks and Their Possible Radiation Hazard, Journal of Agricultural Food Chemistry, 16, 231-234.

Montel, J. (2001) Minerals and design of new waste forms for conditioning nuclear waste. Comptes Rendus Geosciences. 343, 230-236.

Montiel-Rivera, F., Fedoroff, F.M., Jeanjean, J., Minel, L., Barthes, M-G., and Dumonceau, J. (2000) Sorption of selenite on hydroxyapatite: an exchange process. Journal of Colloid and Interface Sciences, 221, 291-2300.

Moore, R.C., Gasser, M., Awwad, N., Holt, K.C., Salas, F.M., Hasan, A., Hasan, M.A., Zhao, H., Sanchez, C.A. (2005) Sorption of plutonium (VI) by hydroxyapatite. Journal of. Radioanalytical and Nuclear Chemistry 263, 97-101.

Moore, R.C., Holt, K., Zhao, H.T., Hasan, A., Awwad, N., Gasser, M., and Sanchez, C. (2003) Sorption of Np(V) by synthetic hydroxyapatite. Radiochimica Acta 91(12). 721-727.

Moore, R.C., Holt, K., Sanchez, C., Zhao, H., Salas, F., Hasan, A., and Lucero, D. (2002) In situ formation of apatite in soil and groundwater for containment of radionuclides and heavy metals. SAND2002-3642. Sandia National Laboratories.

Moore, R.C., Sanchez, C., Holt, K., Zhang, P.C., Xu, H.F., and Choppin, G.R. (2004) Formation of hydroxyapatite in soils using calcium citrate and sodium phosphate for control of strontium migration. Radiochimica Acta 92, 719-723.

Mortvedt, J.J. (1991) Plant and soil relationship of uranium and thorium decay series radionuclides – A Review National Symposium on Naturally Occurring Radionuclides in Agricultural Products, Orlando, FL Jan 24-25.

Murray, F. H., Brown, J. R., Fyfe, W. S., & Kronberg, B. I. (1983) Immobilization of U-Th-Ra in mine wastes by phosphate mineralization. Canadian Mineralogist, 21, 607-610.

Naftz, D.L, Fuller, C.C., Davis, J.A., Piano, M.J., Morrison, S.J., Frethey, G.W., and Rowland, S.C. (2000) Field demonstration of permeable reactive barriers to control uranium contamination in ground water. Presented at the 2nd International Conference on Remediation of Chlorinated and Reacalcitrant Compounds. Monterey, CA May 22-25.

Neuman, W.F., Hursh, J.B., Boyd, J. and Hodge, H.C. (1955) On the mechanism of skeletal fixation of radium. Annals of the New York Academy of Sciences, 62: 125–136.

Narasaraju, T.S.B. and Phebe, D.E., (1996) Some physico-chemical aspects of hydroxyapatite. Journal of Materials Science, 31, 1-21.

Oelkers, E. and Montel, J.M. (2008) Phosphates and nuclear waste storage. Elements 4, 113-116.

Ohnuki, T., N. Kozai, M. Samadfam R. Yasuda, S. Yamamoto, K. Narumi, H. Naramoto and T. Murakamie (2004) The formation of autunite (Ca(UO2)2(PO4)2SnH2O) within the leached layer of dissolving apatite: incorporation mechanism of uranium by apatite. Chemical Geology, 211, 1-14.

Omel'yaneko, I., Livshits, T.S., Yudintsev, B., Nikonov (2007) Natural and artificial matrices for the immobilization of actinides. Geology of Ore Deposits 49, 173-193.

Otton, J.K., Zielinski, R.A., and Horton, R.J. (2010) Geology, geochemistry, and geophysics of the Fry Canyon uranium/copper project site, southeastern Utah – indications of contaminant migration. U.S. Geological Survey Report 2010-5075.

Ouchani, S., Dran, J.C., and Chaumont, J. (1997) Evidence of ionization annealing upon helium-ion irradiation of pre-damaged fluorapatite. Nuclear Instrumentation Methods in. Physics Research. B, 132, 447–451.

Pan, Y., and Fleet, M.E. (2002) Compositions of the apatite-group minerals: Substitution mechanisms and controlling factors. In Kohn, M.J., Rakovan, J., and Hughes, J.M. Eds., Phosphates: Geochemical, Geobiological, and Materials Importance, 48, p. 13–50. Reviews in Mineralogy and Geochemistry, Mineralogical Society of America, Chantilly, Virginia.

Park, H.S., Kim, I.T., Kim, H.Y., Lee, K.S., Rye, S.K. and Kim, J.H. (2002) Application of apatite waste form for the treatment of water-soluble wastes containing radioactive elements. Part 1: investigation on the possibility. Journal of Industrial Engineering Chemistry, 8, 318-327.

Parkhurst, D.L., Appelo, C.A.J. (1999) User's Guide to PHREEQC (Version 2) — A Computer program for speciation, batch-reaction, one-dimensional transport, and inverse geochemical calculations. U.S. Geological Survey.

Phebe D.E., and Narasaraju, T.S.B. (1995) Preparation and characterization of hydroxyl and iodide apatites of calcium and their solid solutions, Journal of Materials Science Letters, 14, 229-231.

Raicevic, S., Vukovi, Z., Lizunova, T.L., and Komarov, V.F. (1996) The Uptake of strontium by calcium phosphate phase formed at an elevated pH. Journal of Radioanalytical and Nuclear Chemistry, 204, 363-370.

Raicevic, S., Wright, J., Veljkovic, V., and Conca, J.L. (2006) Theoretical stability assessment of uranyl phosphates and apatites: selection of amendments for in situ remediation of uranium. Science of the Total Environment 355, 13-24.

Rakovan, J.F., and Pasteris, J.D. (2015) A technological gem: materials, medical, and environmental mineralogy of apatite. Elements, 11, 195-200.

Sasaki, K., Tsuruyama, S., Moriyama, S., Handley-Sidhu, S., Renshaw, J.C., Macaskie, L.E., and Macaskie, E. (2012) Ion exchange capacity of Sr^{2+} onto calcined biological hydroxyapatite and implications for use in permeable reactive barriers. Materials Transactions, 53, 1267-1272.

Seaman, J., Meehan, T., and Bertsch, F. P. (2001) Immobilization of 137Cs and U in contaminated sediments using soil amendments. Journal of Environmental Quality, 30, 1206–1213.

Soulet, S., Carpena, J., Chaumont, J., Krupa, J.C., and Ruault, M.O. (2001) Determination of the defect mechanism in the mono-silicates fluorapatite. Disorder modeling under repository conditions. Journal of Nuclear Materials, 299, 227-234.

Simon, F.G., Biermann, V., and Peplinski, B. (2008) Uranium removal from groundwater using hydroxyapatite. Applied Geochemistry, 23, 2137-2145.

Smiciklas, I., Onjia, A., Markovic, J., and Raicevic, S. (2005) Comparison of hydroxyapatite sorption properties towards cadmium, lead, zinc and strontium ions Current Research in Advanced Materials and Processes, 494, 405-410.

Smiciklas, L.D., Milonjie, S.K., Pfendt, P., and Raicevie, S. (1999) The point of zero charge and sorption of cadmium (II) and strontium (II) ions on synthetic hydroxyapatite. Separation and Purification Technology, 18, 185-194.

Smiciklas, I., Dimovic, S., Plecas, I., and Mitric, M. (2006) Removal of Co^{2+} from aqueous solutions by hydroxyapatite. Water Research, 40, 2267-2274.

Smiciklas, I., Onjia, A., Raicevic, S., Janackovic, D. and Mitric, M. (2008) Factors Influencing the removal of divalent cations by hydroxyapatite. Journal of Hazardous Materials, 152, 876-884.

Thakur, P., Moore, R.C., and Choppin, G.R. (2006) $Np(V)O_2^+$ sorption on hydroxyapatite-effect of calcium and phosphate anions. Radiochimica Acta 94, 645-649.

Terra, O., Audubert, F, Dacheux, N., Guy, C., and Podor, R (2006) Synthesis and characterization of thorium-bearing britholites. Journal of Nuclear Materials, 354, 49-65.

Terra, O., Dacheux, N., Audubert, F., and Podor, R. (2006) Immobilization of tetravalent actinides in phosphate ceramics. Journal of Nuclear Materials, 352, 224-232.

Terra, O., Audubert, F, Dacheux, N., Guy, C., and Podor, R (2007) Immobilization of tetravalent actinides in phosphate ceramics. Journal of Nuclear Materials, 366, 70-86.

Thomson, B.M., Smith, C.L., Busch, R.D., Siegel, M.D., and Baldwin, C. (2003) Removal of metals and radionuclides using apatite and other natural sorbents. Journal of Environmental Engineering 129(6), 492-499.

U.S. Environmental Protection Agency (2007). Monitored natural attenuation of inorganic contaminants in ground water. Volume 3 Assessment for radionuclides including tritium, radon, strontium, technetium, uranium, iodine, radium, thorium, cesium, and plutonium-americium.

Van Haverbeke, L., Vochten, R., and Van Springel, K. (1996) Solubility and spectrochemical characteristics of synthetic chernikovite and meta-ankoleite. Mineralogical. Magazine, 60, 759-766.

Verbeeck, R.M.H., M. Hauben, H.P. Thun, and Verbeeck, F. (1977) Solubility and solution behaviour of strontiumhydroxyapatite. Zeitschriftftir Physikalische Chemie 108, no. 2, 203-215.

Vermuel, V.R., Szecsody J.E., Fritz, B.G., Williams, M.D., Moore, R.C., and Fruchter, J.S. (2014) An injectable permeable reactive barrier for in situ ^{90}Sr immobilization. Groundwater Monitoring and Remediation, 34, p. 28-41.

Wellman, D.M., Glovack, J.N., Parker, K.E., Richards, E.L., and Pierce, E.M. (2008) Sequestration and retention of uranium (VI) in the presence of hydroxylapatite under dynamic geochemical conditions. Environmental Chemistry 5(1), 40-50.

Zhang P., Krumhansl, J.L., and Brady P. V. (2002) Introduction to properties, sources, and characteristics of soil radionuclides. In Geochemistry of soil radionuclides (ed. P. Zhang and P. V. Brady), 1-19. Soil Science Society of America.

Zhang, P.C., and Ryan, J.A. (1998) Formation of pyromorphite in anglesite-hydroxyapatite suspensions under varying pH conditions. Environmental Science and Technology 32:3318–3324.

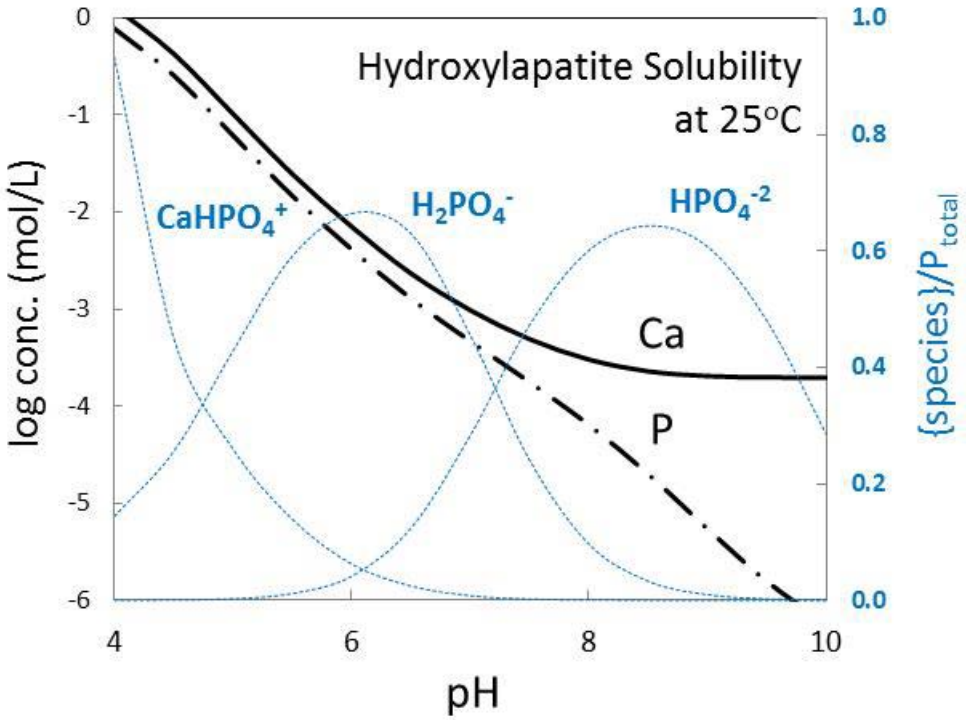

Figure 1. Hydroxyapatite solubility at 25°C in a 100 ppm Na, 100 ppm Cl, 1 ppm P, 10 ppm Ca solution.

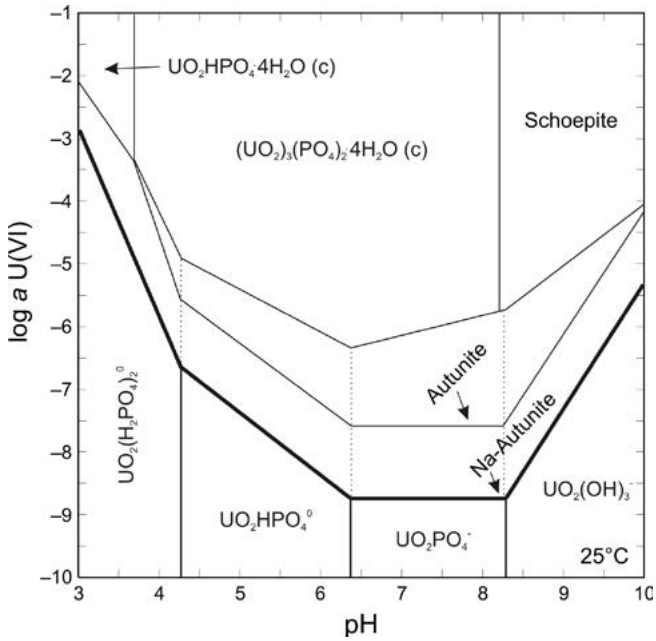

Figure 2. Solubility of U(VI) as a function of pH and in the presence of phosphate ($10^{-3.5}$), sodium (10^{-3}), and calcium (10^{-3}). Dashed lines show the metastable extensions of aqueous U(VI) species (from U.S. Environmental Protection Agency, 2007).

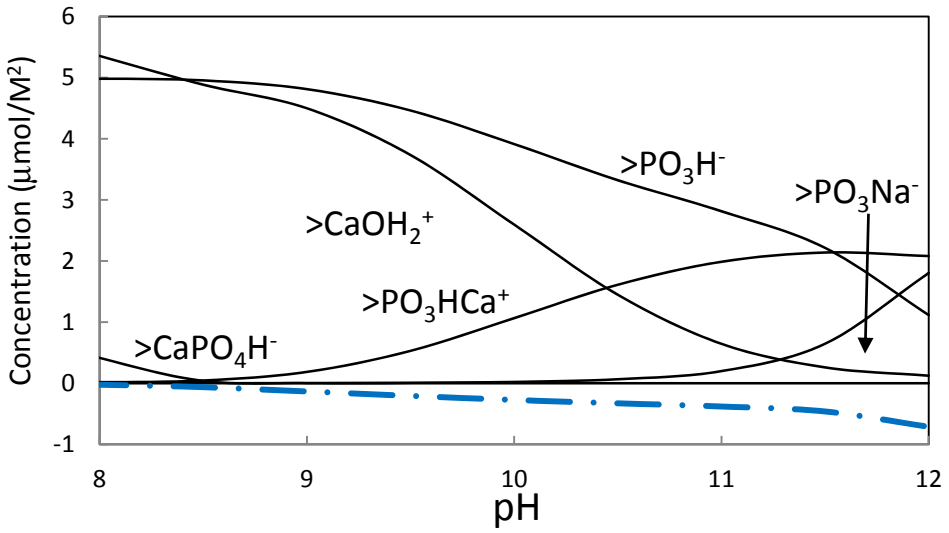

Figure 3. Calculated hydroxyapatite surface speciation in a 2.25 mmol/L Ca and 0.95 mmol/L P solution. The net hydroxyapatite surface charge is plotted in dashed-dot blue. Ca and P surface site densities were assumed to be respectively 4.3 and 3 sites/nm^2 (Bengtsson, Shchukarev Persson, P, and Sjöberg, S 2008).

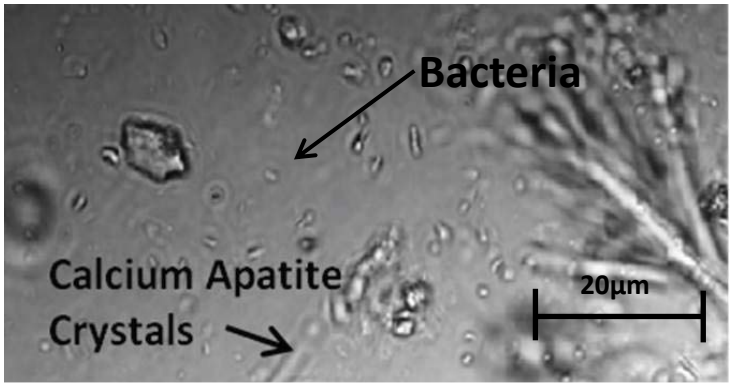

Figure 4. Crystals of apatite formed using an aqueous solution of sodium phosphate and calcium citrate in

Table 1. Common Soil/Radwaste Radionuclides (after Zhang et al. 2002)

Radionuclide	**Half-life (yrs)**	**Notes**
^{90}Sr	29	Fallout, nuclear processing, accidental releases
^{137}Cs	30.2	Fallout, nuclear processing, accidental releases
^{129}I	16,000,000	Nuclear processing
^{226}Ra	1600	Uranium decay
$^{234,235,238}U$	250,000,700 million, 4.5 billion	Natural, spent fuel & processing
$^{239,240,241}Pu$	24000, 6560, 14.4	Fallout, accidental releases
^{60}Co	5.3	Low-level radioactive waste
^{241}Am	432.2	Spent fuel & processing, sealed sources (e.g. smoke detectors)
^{99}Tc	213,000	Fission product, nuclear processing
Th	several	Radioactive decay, processing

Table 2. Metal- and radionuclide-phosphate hydrolysis reactions (from the data0.ymp.R2 thermodynamic database).

Mineral	**Formula**	**Log K_{25C}**
Hydroxyapatite	$Ca_5(OH)(PO_4)_3 + 4H^+ \leftrightarrow 5Ca^{+2} + 3HPO_4^{-2} + H_2O$	0.5251
	$SrHPO_4 \leftrightarrow Sr^{+2} + HPO_4^{-2}$	-8.5400
	$(UO_2)_3(PO_4)_2 + 2H^+ \leftrightarrow 3UO_2^{+2} + 2HPO_4^{-2}$	-11.5914
	$(UO_2)_3(PO_4)_2{:}4H_2O + 2H^+ \leftrightarrow 3UO_2^{+2} + 2HPO_4^{-2} + 4H_2O$	-24.2808
	$(UO_2)_3(PO_4)_2{:}6H_2O + 2H^+ \leftrightarrow 3UO_2^{+2} + 2HPO_4^{-2} + 6H_2O$	-25.4205
	$U(HPO_4)_2{:}4H_2O \leftrightarrow U^{+4} + 2HPO_4^{-2} + 4H_2O$	-30.4577
	$UO_2HPO_4{:}4H_2O \leftrightarrow UO_2^{+2} + HPO_4^{-2} + 4H_2O$	-2.2729
	$UPO_5 + H_2O \leftrightarrow UO_2^{+} + + H^+ + HPO_4^{-2}$	-18.3752
	$Pu(HPO_4)_{2,am,hyd} \leftrightarrow Pu^{+4} + 2HPO_4^{-2}$	-30.4500
	$PuPO_{4,hyd} + H^+ \leftrightarrow Pu^{+3} + HPO_4^{-2}$	-12.2500
	$Th_{0.75}PO_4 + H^+ \leftrightarrow Th^{+4} + HPO_4^{-2}$	-15.6495
	$AmPO_{4,am} + H^+ \leftrightarrow Am^{+3} + HPO_4^{-2}$	-12.4399
	$Co_3(PO_4)_2 + 2H^+ \leftrightarrow 3Co^{+2} + 2HPO_4^{-2}$	-10.0036
	$CoHPO_4 \leftrightarrow Co^{+2} + HPO_4^{-2}$	-6.7187

Table 3. Hydroxyapatite surface complexation model (Brady et al., 2014).

Surface Reaction	**Log K_{25C}**
$>CaOH + H^+ \leftrightarrow >CaOH_2^+$	8.41
$>PO_3H_2 \leftrightarrow >PO_3H^- + H^+$	-1.11
$>CaOH + HPO_4^{-2} + H^+ \leftrightarrow >CaPO_4H^- + H_2O$	11.63
$>PO_3H_2 + Na^+ \leftrightarrow >PO_3Na^- + 2H^+$	-5.1
$>PO_3H_2 + Ca^{+2} \leftrightarrow >PO_3HCa^+ + H^+$	-0.7
$>PO_3H_2 + Mg^{+2} \leftrightarrow >PO_3HMg^+ + H^+$	-0.7